Numerical Study of the Axial and Radial Forces, the Stresses and the Strains in a High Pressure Multistage Centrifugal Pump

Mohand-Amokrane Abdelouahab[1], Guyh Dituba Ngoma[1], Fouad Erchiqui[1] and Python Kabeya[2]
[1]*University of Quebec in Abitibi-Témiscamingue, School of Engineering's Department, 445, Boulevard de l'Université, Rouyn-Noranda, Quebec, J9X 5E4, Canada*
[2]*University of Kinshasa, Department of Mechanical Engineering, Kinshasa, Democratic Republic of the Congo*

Keywords: Multistage Centrifugal Pump, Axial and Radial Forces, Stress, Strain, CFX, Static Structural Analysis.

Abstract: This paper deals with the numerical study of the axial and radial forces, the stresses and the strains induced by a liquid flow in a high pressure multistage centrifugal pump to improve their performances account for the material of the shaft and the impellers. Indeed, a model of a 4-stage centrifugal pump is developed considering a design point. The continuity and the Navier-Stokes equations are used for the liquid flow through the pump. Additionally, the equations of the stresses and the strains are applied for the shaft and the impellers. The obtained system of equations is solved by means of the CFX-code and the static structural analysis to determinate the fields of velocity and pressure, the axial and radial forces, the stress and the strain on the pump shaft. Moreover, numerical simulations are carried out to analyze the shaft behavior in terms of the induced axial and radial forces, the stresses and the strains. The diffuser in the last pump stage is used as parameter. Good trends are achieved comparing the obtained results with these found in the literature and these calculated using the classical equations of the stresses and the strains.

1 INTRODUCTION

The growing technological development in the field of liquid transportation in the mining sector is leading pump manufacturers to design and develop high pressure multistage centrifugal pumps that are continually adapted to the industrial needs. Its operation and its adequate life expectancy greatly depend on the design and manufacture of its components, such as, inter alia, the shaft, the bearings, the impellers and the diffusers.

To better design and optimize the pump shaft and the bearings of the multistage centrifugal pumps, the axial and the radial forces acting on the impellers must be known with accuracy to determinate the bearing loads, the shafts stresses and the shaft deflection accounting for the entire flow range. This allows to avoid, mainly, the excessive bending of the pump shaft, too high stresses on the pump shaft, and the overloading of the axial and radial bearings. In fact, several theoretical and experimental research works have been done on the multistage centrifugal pumps in the terms of the axial and radial forces, the stresses and the strains acting on the pump shaft (Karassik and McGuire, 1998; Gülich, 2010; Wang et al., 2013; Watanabe, 2019; Gantar et al., 2002; Bolade and Madki, 2015; TM.P. S.p.A. Termomeccanica Pompe, 2003; Karassik et al., 2008; Wang et al., 2014; and Suke et al., 2015).

In most previous study on the multistage centrifugal pumps, the effects of the induced axial and radial loads, the stresses and the strains accounting for the diffuser return vanes and the diffuser in the last pump stage in relation to the pump head, the brake horsepower and the efficiency have been less investigated (Jino, T., 1980). Since the pump performances of the multistage centrifugal pumps depend, among other things, on the design of the diffuser including the return vanes (Miyano et al., 2008; and La Roche-Carrier et al., 2013), this is essential to consider also the impact of the diffuser on the axial and radial forces, the stresses and the strains on the pump shaft.

Therefore, this research is focused to the development of reliable and accurate numerical models of a high pressure multistage centrifugal

Abdelouahab, M., Ngoma, G., Erchiqui, F. and Kabeya, P.
Numerical Study of the Axial and Radial Forces, the Stresses and the Strains in a High Pressure Multistage Centrifugal Pump.
DOI: 10.5220/0009783001810188
In *Proceedings of the 10th International Conference on Simulation and Modeling Methodologies, Technologies and Applications (SIMULTECH 2020)*, pages 181-188
ISBN: 978-989-758-444-2

pump in order to study in-depth the axial and radial forces, the stresses and the strains on the pump shaft due to the liquid flow through the pump at varying operating conditions using the 4-stage centrifugal pump and the diffuser in the last pump stage as parameter in relation to the pump performances.

The achieved results using two diffuser types for the pump head, the brake horsepower and the efficiency are compared. Furthermore, considering the first pump stage, a good trend is obtained validating the numerical results for the stresses on the pump shaft from the determined axial and radial forces by means of the classical equations of the strength of materials and the mechanical design of machine elements.

2 MODEL DESCRIPTION

Fig. 1 illustrates the components of the reference 4-stage centrifugal pump considered in this study. It is mainly composed of a shaft, four impellers and four diffusers. The solid and fluid models of the 4-stage centrifugal are shown in Fig. 2.

a) Shaft, impellers and diffuser with return vanes of type 1.

b) Pump stages: impeller and diffuser combined.

Figure 1: Components of a 4-stage centrifugal pump (School of Engineering's Department, Turbomachinery laboratory, E-216, www.uqat.ca).

a) Solid model

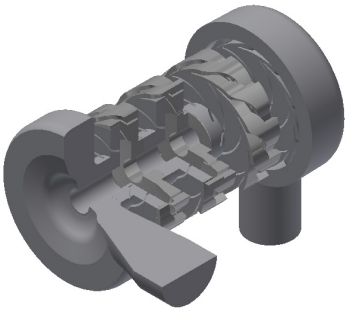

b) Fluid model

Figure 2: 4-stage centrifugal pump models (Abdelouahab M.-A., 2018).

Furthermore, relating to the pump diffuser, there are some multistage centrifugal pumps that use another type of the diffuser (La Roche-Carrier et al., 2013) as indicated in Fig. 3. The performance comparison of both diffuser types are done in this work.

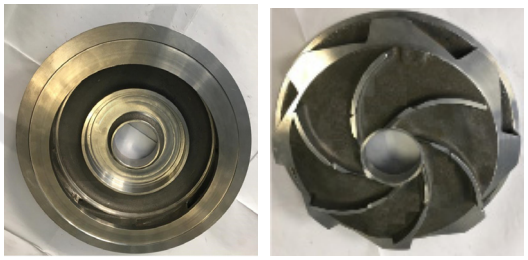

a) Technosub Inc., www.technosub.net.

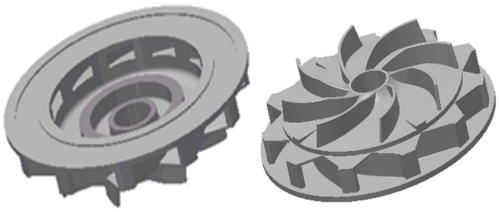

b) Diffuser solid model.

Figure 3: Diffuser with return vanes of type 2.

3 GOVERNING EQUATIONS

To determinate the fields of liquid flow velocity and pressure in a multistage centrifugal pump, the following hypotheses are considered (La Roche-Carrier et al., 2013): (a) a steady state, three-dimensional and turbulence flow using the k-ε model is assumed; (b) the liquid is an incompressible liquid; (c) it is a newtonian liquid; and (d) the liquid's thermophysical properties are constant with the temperature.

Additionally, for the equations that govern the solid mechanics for the calculation of the stresses and the strains in the multistage centrifugal pump, the applied assumptions are formulated as follows (Popov, 1999): (i) the material is considered continuous, doesn't have cracks, nor cavities; (ii) the material is homogeneous and presents the same properties in all points; (iii) the material is considered as isotropic; and (iv) no internal force acts in the material before the application of the external loads.

3.1 Liquid Flow Velocity and Pressure

The fields of liquid flow velocity and pressure are found resolving the equations of the continuity and the Navier-Stokes accounting for the corresponding assumptions and using the ANSYS CFX-code (ANSYS inc.), based on the finite volume method (La Roche-Carrier et al., 2013). The boundary conditions are formulated as follows: the static pressure is given at the pump inlet, while the flow rate is specified at the pump outlet. The frozen rotor condition is used for the impeller-diffuser interface per pump stage. A no-slip condition is set for the flow at the wall boundaries.

Applying the coordinate system, the equations of the continuity are given by:

$$\frac{\partial u}{\partial x}+\frac{\partial v}{\partial y}+\frac{\partial w}{\partial z}=0 \tag{1}$$

where u(x,y,z), v(x,y,z) et w(x,y,z) are components of the liquid flow velocity in the direction x, y and z.

Moreover, the equations of the Navier-Stokes are expressed by:

$$\begin{aligned}
\rho\left(u\frac{\partial u}{\partial x}+v\frac{\partial u}{\partial y}+w\frac{\partial u}{\partial z}\right)&=\mu_{eff}\left(\frac{\partial^2 u}{\partial x^2}+\frac{\partial^2 u}{\partial y^2}+\frac{\partial^2 u}{\partial z^2}\right)\\
&\quad-\frac{\partial p}{\partial x}+\rho(\omega_z^2 r_x+2\omega_z v)\\
\rho\left(u\frac{\partial v}{\partial x}+v\frac{\partial v}{\partial y}+w\frac{\partial v}{\partial z}\right)&=\mu_{eff}\left(\frac{\partial^2 v}{\partial x^2}+\frac{\partial^2 v}{\partial y^2}+\frac{\partial^2 v}{\partial z^2}\right)\\
&\quad-\frac{\partial p}{\partial y}+\rho(\omega_z^2 r_y-2\omega_z u)\\
\rho\left(u\frac{\partial w}{\partial x}+v\frac{\partial w}{\partial y}+w\frac{\partial w}{\partial z}\right)&=\mu_{eff}\left(\frac{\partial^2 w}{\partial x^2}+\frac{\partial^2 w}{\partial y^2}+\frac{\partial^2 w}{\partial z^2}\right)\\
&\quad-\frac{\partial p}{\partial z}
\end{aligned} \tag{2}$$

where p is the pressure; ρ is the density; μ_{eff} is the effective viscosity accounting for turbulence, it is defined as $\mu_{eff}=\mu+\mu_t$. μ is the dynamic viscosity and μ_t is the turbulence viscosity. It is linked to turbulence kinetic energy k and dissipation ε.

The k-ε turbulence model is used in this work due to the better convergence than with other turbulence models.

To determinate the performance parameters of the multistage centrifugal pump, the pump head is described as $H=(p_{to}-p_{ti})/\rho g$, where p_{ti} is the total pressure at the pump inlet and p_{to} the total pressure at the pump outlet. The hydraulic power of the pump is formulated as $P_h=\rho QgH$, where Q is the flow rate. Moreover, the brake horsepower of the pump is given by $P_s=T\omega$, where T is the impeller torque and ω is the angular velocity. From the hydraulic power and the brake horsepower, the efficiency of the pump can be expressed as $\eta=P_h/P_s$.

3.2 Axial and Radial Forces

The axial forces is the result of unbalanced impeller forces acting in the shaft axial direction. It is composed of the force on the impeller's front shroud and hub shroud due to the static pressures on the surface areas of the shrouds, and the momentum force due to the change in direction of the liquid flow through the impeller.

Furthermore, the radial force on the impeller results from a non-uniform distribution of pressure on the circumference of the impeller. The non-uniform pressure distribution can be caused by: the geometrical form of the diffuser for the multistage centrifugal pumps; the non-symmetrical impeller inflow; or the pump operating regime. It is to highlight that the radial force depends on the time. Its components are the static radial force and the dynamic radial force. Generally, the static radial force is greater than the dynamic radial force (Karassik and McGuire, 1998; Gülich, 2010; Wang et al., 2013;

Watanabe, 2019; Gantar et al., 2002; Bolade and Madki, 2015;TM.P. S.p.A. Termomeccanica Pompe, 2003; Karassik et al., 2008; Jino, T., 1980; Abdelouahab M.-A., 2018).

In this research, the axial and radial forces due to the liquid flow through the multistage centrifugal pump are determined using the ANSYS CFX-code.

3.3 Stress and Strains

The fundamental principles of the strength of materials are accounted for the resolution of the solid mechanics equations (Popov, 1999): the superposition principle and the Saint-Venant principle. The method of resolution of the structural problems in the solid mechanics consists of three steps: (i) the force analysis forces and the equilibrium conditions; (2) the study of the displacements and the geometric accounting; and (iii) the application of the relations of forces and displacements.

Neglecting the forces per unit of volume, the equilibrium equations of elasticity in terms of three normal and three shear stress components are expressed by:

$$\begin{aligned}\frac{\partial\sigma_x}{\partial x}+\frac{\partial\tau_{yx}}{\partial y}+\frac{\partial\tau_{zx}}{\partial z}=0\\ \frac{\partial\tau_{xy}}{\partial x}+\frac{\partial\sigma_y}{\partial y}+\frac{\partial\tau_{zy}}{\partial z}=0\\ \frac{\partial\tau_{xz}}{\partial x}+\frac{\partial\tau_{yz}}{\partial y}+\frac{\partial\partial_z}{\partial z}=0\end{aligned} \tag{3}$$

Furthermore, the principal stresses, designed as σ_1, σ_2 and σ_3, are calculated from the σ_x, σ_y, σ_z, τ_{xy}, τ_{xz} and τ_{yz}. They are the invariants. Its values do not depend on the orientation of the part with respect to the xyz coordinate system. It is to highlight that the principal stresses are available as individual result. They are ordered such that $\sigma_1 > \sigma_2 > \sigma_3$. These can be given by:

$$\begin{aligned}\sigma_1=\sigma_0+2\left(\left|\frac{J_2}{3}\right|\right)^{\frac{1}{2}}\cos\left(\frac{1}{3}\arccos\left(-0.5J_3\left(\left|\frac{J_2}{3}\right|\right)^{-1.5}\right)\right)\\ \sigma_2=\sigma_0-2\left(\left|\frac{J_2}{3}\right|\right)^{\frac{1}{2}}\cos\left(\frac{1}{3}\arccos\left(-0.5J_3\left(\left|\frac{J_2}{3}\right|\right)^{-1.5}\right)+\frac{\pi}{3}\right)\\ \sigma_3=\sigma_0-2\left(\left|\frac{J_2}{3}\right|\right)^{\frac{1}{2}}\cos\left(\frac{1}{3}\arccos\left(-0.5J_3\left(\left|\frac{J_2}{3}\right|\right)^{-1.5}\right)-\frac{\pi}{3}\right)\end{aligned} \tag{4}$$

where

$$\begin{aligned}\sigma_0&=\frac{1}{3}\left(\sigma_x+\sigma_y+\sigma_z\right)\\ J_2&=s_xs_y+s_ys_z+s_zs_x-\tau_{xy}^2-\tau_{yz}^2-\tau_{zx}^2\\ J_3&=-\left(s_xs_ys_z-s_x\tau_{yz}^2-s_y\tau_{zx}^2-s_z\tau_{xy}^2\right)\\ s_x&=\sigma_x-\sigma_0;\ \ s_y=\sigma_y-\sigma_0;\ \ s_z=\sigma_z-\sigma_0\end{aligned} \tag{5}$$

Moreover, concerning the normal strains (ε_x, ε_y and ε_z) and the shear strains (γ_{xy}, γ_{yz} and γ_{zx}), they can be written as:

$$\begin{aligned}\varepsilon_x=\frac{\partial u}{\partial x};\ \ \varepsilon_y=\frac{\partial v}{\partial z};\ \ \varepsilon_z=\frac{\partial w}{\partial z}\\ \gamma_{xy}=\frac{\partial u}{\partial x}+\frac{\partial u}{\partial y};\ \ \gamma_{yz}=\frac{\partial w}{\partial y}+\frac{\partial v}{\partial z};\ \ \gamma_{zx}=\frac{\partial u}{\partial z}+\frac{\partial w}{\partial x}\end{aligned} \tag{6}$$

where u, v and w are the displacements respectively in the directions of x, y and z.

In addition, for the relationships between the stresses and the strains, the generalized Hook's law for isotropic materials is used:

$$\begin{aligned}\varepsilon_x&=\frac{1}{E}\left[\sigma_x-\nu(\sigma_y+\sigma_z)\right]\\ \varepsilon_y&=\frac{1}{E}\left[\sigma_y-\nu(\sigma_z+\sigma_x)\right]\\ \varepsilon_z&=\frac{1}{E}\left[\sigma_z-\nu(\sigma_x+\sigma_y)\right]\\ \gamma_{xy}&=\frac{\tau_{xy}}{G};\ \ \gamma_{yz}=\frac{\tau_{yz}}{G};\ \ \gamma_{zx}=\frac{\tau_{zx}}{G}\end{aligned} \tag{7}$$

where E is the modulus of elasticity, G is the shear modulus and ν is the Poisson's ratio.

Inversely, the stresses can be expressed by:

$$\begin{aligned}\sigma_x&=\frac{E}{(1+\nu)(1-2\nu)}\left[(1-\nu)\varepsilon_x+\nu(\varepsilon_y+\varepsilon_z)\right]\\ \sigma_y&=\frac{E}{(1+\nu)(1-2\nu)}\left[(1-\nu)\varepsilon_y+\nu(\varepsilon_z+\varepsilon_x)\right]\\ \sigma_z&=\frac{E}{(1+\nu)(1-2\nu)}\left[(1-\nu)\varepsilon_z+\nu(\varepsilon_x+\varepsilon_y)\right]\\ \tau_{xy}&=G\gamma_{xy};\ \ \tau_{yz}=G\gamma_{yz};\ \ \tau_{zx}=G\gamma_{zx}\end{aligned} \tag{8}$$

The stress according to von Mises is selected for the yield criteria. This stress is written as follows:

$$\sigma'=\sqrt{\frac{1}{2}\left(\left(\sigma_1-\sigma_2\right)^2+\left(\sigma_2-\sigma_3\right)^2+\left(\sigma_3-\sigma_1\right)^2\right)} \tag{9}$$

For the calculation of the stresses and strains, the ANSYS-code for the structural static analysis is used.

4 RESULTS AND DISCUSSION

Two cases are selected for examination of the shaft behavior of a multistage centrifugal pump with particular emphasis on the axial and radial forces, the

stresses and the strains due to the liquid flow through the pump. The impact of the diffuser in the last pump stage on the shaft is analyzed in different operating conditions in terms of the flow rates.

Tabs. 1-4 indicate the reference data used for the impeller, the diffuser and the shaft. The rotation speed of the shaft is 1800 rpm and the flow rate range is from 300 m³/h to 900 m³/h.

Table 1: Reference data of the impeller.

Inlet blade height b_1 [mm]	56
Outlet blade height b_2 [mm]	44,25
Hub diameter D_{h1} [mm]	84,84
Inlet diameter D_{h2} [mm]	194,95
Outlet diameter D_2 [mm]	401,3
Inlet blade angle β_{b1} [°]	18
Outlet blade angle β_{b2} [°]	22,5
Blade thickness e [mm]	7,94
Blade number Z_b	6

Table 2: Reference data of the diffuser (front side).

Inlet blade height b_3 [mm]	41,98
Outlet blade height b_4 [mm]	68,4
Inlet diameter D_3 [mm]	401,3
Outlet diameter D_4 [mm]	459
Inlet blade angle α_{3b} [°]	16,44
Blade thickness e_3 [mm]	6,04
Blade number Z_{Le}	11

Table 3: Reference data of the diffuser (rear side).

Return vane number Z_R	11
Outlet return vane height b_5 [mm]	24,4
Diameter at the inlet of the return vane D_3 [mm]	459
Blade angle at the inlet of the return vane α_5 [°]	17,04
Blade angle at the outlet of the return vane α_6 [°]	93,84
Blade thickness of the return vane e_3 [mm]	6,04

Table 4: Reference data of the shaft.

Length L [mm]	1000
Diameter d [mm]	71,12

Furthermore, the properties of the standard steel and the water considered are indicated in Tabs. 5 and 6.

Table 5: Properties of the standard steel.

Module of the Young [Pa]	$2x10^{11}$
Poisson ratio	0,3
Compressibility module [Pa]	$1,6667x10^{11}$
Shear module [Pa]	$7,6923x10^{11}$
Resistance coefficient [Pa]	$9,2x10^{8}$
Ductility coefficient [Pa]	10^{9}
Yield strength [Pa]	$2,5x10^{8}$
Ultimate tensile strength [Pa]	$4,6x10^{8}$
Density [kg/m³]	7850

Table 6: Properties of water in 25 °C.

Density [kg/m³]	Thermal expansion coefficient [K⁻¹]	Kinematic viscosity [m²/s]
997	$2,57x10^{-1}$	$0,884x10^{-6}$

4.1 Case Study

4.1.1 Effect of the Flow Rate

To analyze the effect of the flow rate on the radial forces, the stresses and the strains on the shaft of the 4-stage centrifugal pump, the flow rate from 300 m³/h to 900 m³/h are selected keeping the reference data as constant.

Figs. 4-9 show the pump head, the brake horsepower, the efficiency, the radial force, the stress and the strain as a function of the flow rate. From these figures, it is observed that the radial force decreases and increases with growing flow rate. It is the lowest in the best efficiency point (BEP) or in the best efficiency zone, as indicated in Fig. 4. This can be explain by the fact that the impeller is designed for constant velocity near the best efficiency flow rate, which yields an uniform static pressure around the periphery of the impeller, at this flow rate. However, as the flow rate moves away from the BEP, the pressure distribution around the impeller changes, resulting in high radial loads on the pump bearings.

Relating to the stress on the pump shaft, it decreases, then it increases with rising flow rate. The strain follows the same trend as the stress. At the low flow rate and the high flow rate, the radial load on the pump shaft is greater, this can lead to important stress and the strain on the pump shaft. Thus, Figs. 4-9 are relevant to better understanding the relationship between the pump performances and the radial forces, the stresses and the strains on the pump shat.

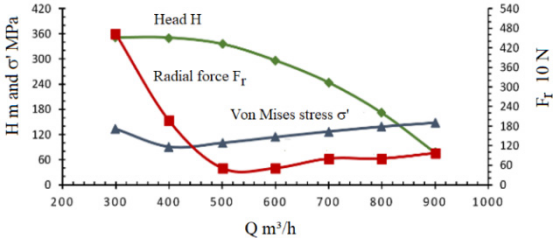

Figure 4: Head, stress, and radial force versus flow rate.

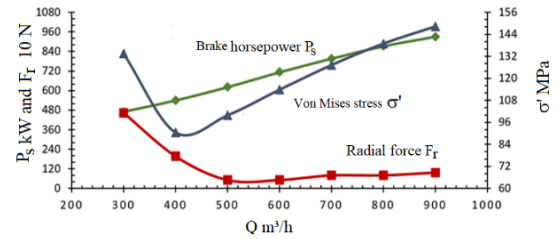

Figure 5: Brake horsepower, stress, and radial force versus flow rate.

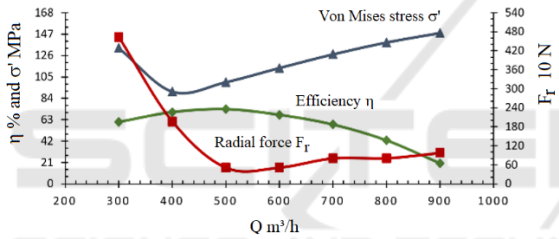

Figure 6: Efficiency, stress, and radial force versus flow rate.

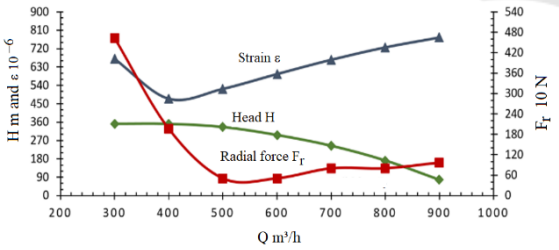

Figure 7: Head, strain, and radial force versus flow rate.

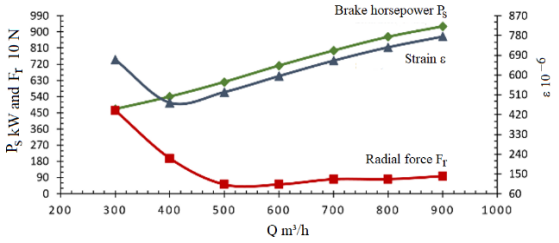

Figure 8: Brake horsepower, strain, and radial force versus flow rate.

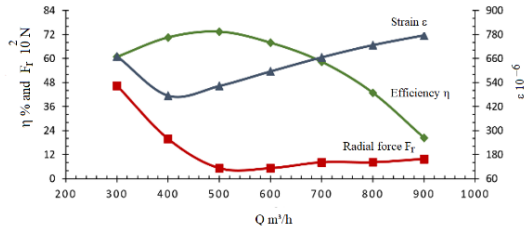

Figure 9: efficiency, strain, and radial force versus flow rate.

4.1.2 Effect of the Diffuser in the Last Pump Stage

To analyze the effect of the diffuser in the last pump stage on the axial and radial forces on the shaft, two models of the 4-stage centrifugal pump are selected whose one having a diffuser in the last pump stage.

The reference data are kept as constant. Figs. 10-14 present the pump head, the brake horsepower, the efficiency, and the axial force and radial forces as a function of the flow rate.

Fig. 10 indicates that the pump head with a diffuser in the last pump stage is greater than the without diffuser case. This can be explained by the fact that a diffuser provides greater static pressure. Moreover, it can be observed in Fig. 11 that the brake horsepower for both cases is practically identical, whereas the efficiency for the case of the last pump stage with the diffuser is relatively higher than the without diffuser case as shown in Fig. 12.

Relating to the axial force, it can be seen that the use of the last pump stage without diffuser leads to the greater axial force as illustrated in Fig. 13. In addition, Fig. 14 presents the fact that the radial force for the case of the last pump stage with the diffuser is higher than the without diffuser case from 300 m³/h to about 460 m³/h, whereas the radial force for the case with the diffuser is lower than the without diffuser case for the flow rate more than 460 m³/h.

Thus, the in-depth knowledge of the resulting axial and radial forces acting on the shaft impellers of the multistage centrifugal pump is essential to better design and to optimize the shat bearings accounting for the last pump stage configuration.

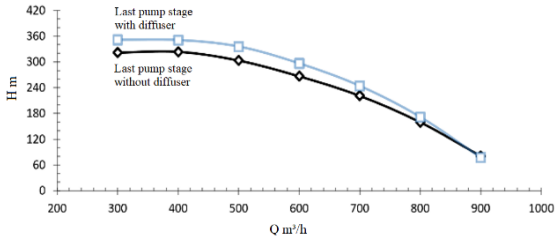

Figure 10: Head versus flow rate.

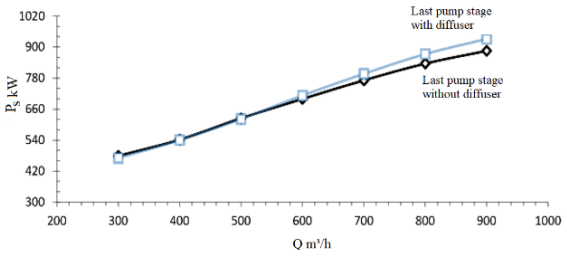

Figure 11: Brake horsepower versus flow rate.

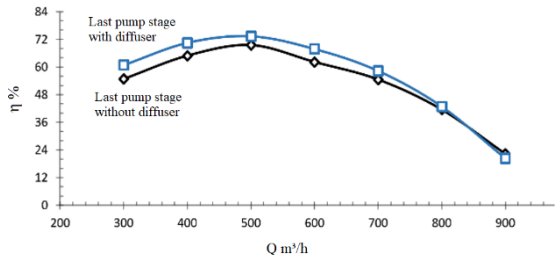

Figure 12: Efficiency versus flow rate.

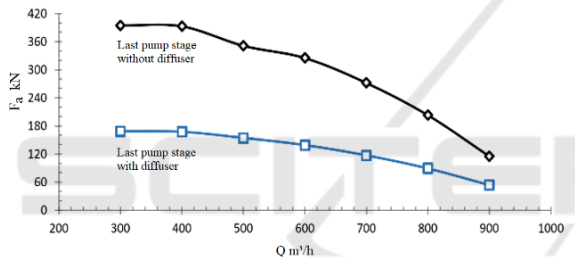

Figure 13: Axial force versus flow rate.

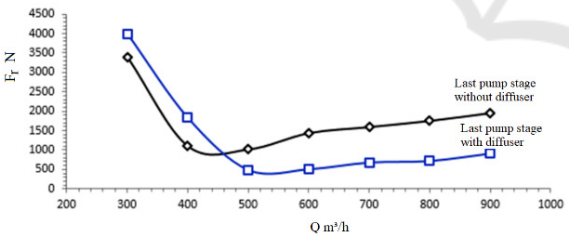

Figure 14: Radial force versus flow rate.

4.2 Comparison of the Results

4.2.1 Pump Performances According to the Diffuser Type

The results of the pump head, the brake horsepower and the efficiency relating to the diffuser of type 1 in Fig. 1 are compared with the obtained results using the diffuser of type 2 in Fig. 3.

Fig. 15 shows that the head achieved of the diffuser in Fig. 1 is higher than that obtained with the diffuser in Fig. 2 for the flow rate from 300 m³/h to about 660 m³/h. Furthermore, Fig. 16 indicates that the brake horsepower for the flow rate from 300 m³/h to 900 m³/h for the diffuser in Fig. 1 are the highest.

In addition, the efficiency for the diffuser in Fig. 2 is better as depicted in Fig. 17. This comparison is relevant to illustrate that the performances of a multistage centrifugal pump can depend, inter alia, on the used diffuser type.

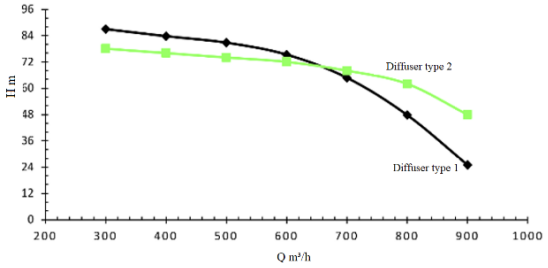

Figure 15: Head versus flow rate.

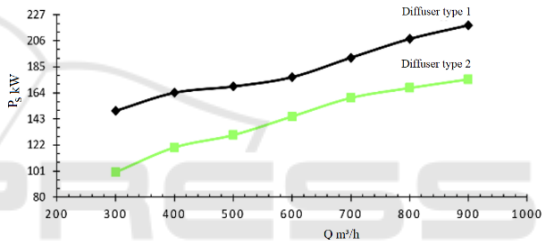

Figure 16: Brake horsepower versus flow rate.

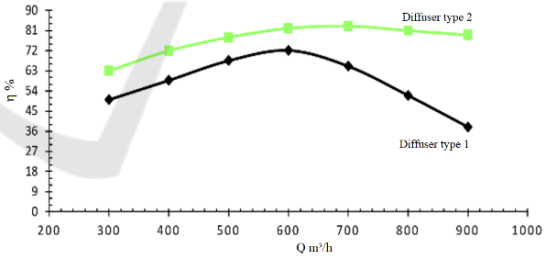

Figure 17: Efficiency versus flow rate.

4.2.2 Stress Results

The results of numerical simulations for the stresses in this study are compared with the results for the stresses using the classical equation for the first pump stage. While confronting the curves in Fig. 18, the trend of the classical and the numerical results are similar. The gaps between the curves can be justified by the different hypotheses used in terms of classical calculations and numerical simulations.

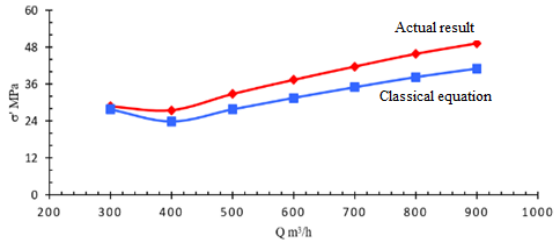

Figure 18: Stress versus flow rate.

5 CONCLUSION

This study focused on the numerical investigation of the axial and radial forces, the stresses and the strains on the shaft of a multistage centrifugal pump due to the liquid flow through this pump. The continuity and the Navier-Stokes equations are used for the liquid flow in the pump. Moreover, the equations of the stresses and the strains are applied for the shaft and the impellers. The ANSYS CFX-code and the static structural analysis code are used to determinate, respectively, the fields of velocity and pressure for the liquid flow, and the axial and radial forces, the stresses and the strains for the shaft. Numerical simulations are accomplished to examine the shaft behavior in terms of the axial and radial forces acting in the impellers, the stresses and the strains on the shaft. For these simulations, inter alia, the diffuser in the last pump stage is considered as parameter. This is to find a relevant relationship between the pump performances, the axial and radial loads, the stresses and the strain on the shaft. The numerical results for the pump performances using two diffuser types are compared. In addition, the obtained numerical results for the stresses on the shaft are validated considering the first pump stage by means of the results found applying the classical equations.

ACKNOWLEDGMENTS

The authors are grateful to the Technosub Inc., Industrial pumps manufacturing and distribution (Rouyn-Noranda, Quebec, Canada).

REFERENCES

Karassik, I. J., McGuire, T., 1998. *Centrifugal Pumps*. Springer-Verlag US.

Gülich, J. F., 2010. *Centrifugal Pumps*, second Edition, Springer.

Wang C., Shi, W. and Zhang, L., 2013. Calculation Formula Optimization and Effect of Ring Clearance on Axial Force of Multistage Pump. *Hindawi Publishing Corporation, Mathematical Problems in Engineering*, Vol. 2013, Article ID 749375.

Watanabe, H., 2019. Prediction of flow phenomena, performance and thrust forces of three-stage pump by using URANS. *IOP Conf. Series: Earth and Environmental Science 240*.

Gantar M., Florjancic D., and Sirok B., 2002. Hydraulic Axial Thrust in Multistage Pumps - Origins and Solutions. *Journal Fluids Engineering*, Vol. 124, Issue 2, 336-341, 6 pages.

Bolade, P. S., Madki, S. J., 2015. Analysis of Hydraulic Thrusts in Centrifugal Pump to Increase the Bearing Life. *International Journal of Engineering Research & Technology*. ISSN: 2278-0181, Vol. 4 Issue 08.

TM.P. S.p.A. Termomeccanica Pompe, 2003. *TERMOMECCANICA Centrifugal pump handbook*, La Spezia – Italy.

Karassik, I. J., Messina, J. P., Cooper, P., Heald, C. C., 2008. *Pump Handbook*. Fourth edition McGRAW-HILL.

Wang, C., Shi, W., Si, Q., Zhou, L., 2014. Numerical calculation and finite element calculation on impeller of stainless steel multistage centrifugal pump. *Journal of Vibroengineering*, Vol. 16, Issue 4, p. 1723-1734.

Suke, A. C., Londhe, B. P., Verma, A. B., 2015. Shaft deflection Analysis of Multistage centrifugal Pump by Finite element Method. *International Journal of Science, Engineering and Technology Research*, Vol. 4, Issue 7.

Jino, T., 1980. Hydraulic axial thrust in multistage centrifugal pumps. *Journal of Fluids Engineering*, Volume 102, Issue 1, 6 pages.

Miyano, M., Kanemoto, V, Kawashima, D., Wada, A., Hara, T., and K. Sakoda, K., 2008. Return vane installed in multistage centrifugal pump. *International Journal of Fluid Machinery and Systems*, vol. 1, no. 1, pp. 57–63.

La Roche-Carrier N., Dituba Ngoma G., and Ghie W., 2013. Numerical investigation of a first stage of a multistage centrifugal pump: impeller, diffuser with return vanes, and casing. *ISRN Mechanical Engineering*, Vol. 2013, Article ID 578072, 15 pages.

School of Engineering's Department, Turbomachinery laboratory (E-216), University of Quebec in Abitibi-Témiscamingue (UQAT), www.uqat.ca.

Abdelouahab M.-A., 2018. *Étude des contraintes, vibrations, poussées axiales et radiales induites par des écoulements des liquides complexes dans une pompe centrifuge multi-étage à grande pression et puissance*. Mémoire de mâitrise, Université du Québec en Abitibi-Témiscamingue.

Popov E. P., 1999. *Engineering Mechanics of Solids*, 2nd edition, Prentice Hall.

Technosub Inc., www.technosub.net.

ANSYS inc., www.ansys.com.